Proceedings of 7th International Conference on Squeezed States and Uncertainty Relations

Quantum filtering by two-photocurrent devices

Matteo G A Paris
QUANTUM OPTICS & INFORMATION GROUP
Istituto Nazionale per la Fisica della Materia, Unitá di Pavia, Italia

We address the characterization of optical signals by means of detectors that jointly measure a pair of photocurrents, *i.e* detectors that couples the mode under examination with a suitably prepared probe mode. The complete equivalence of three different such detectors: heterodyne, eight-port homodyne and six-port homodyne detectors is established, both for ideal conditions and for realistic working regimes, *i.e.* in presence of losses or for not fully efficient photocounters. We evaluate the output statistics for a generic probe mode, and briefly illustrate the use of two-photocurrent devices to the characterization of optical signals via *quantum filtering*.

I. INTRODUCTION

In order to gain information about a quantum state of radiation one has to measure some observable. The measurement process unavoidably involves some kind of interaction, which couples the mode under examination (the signal) to one or more other modes of the field (hereafter referred to as the probe). Therefore, one has to admit that, in general, the measured observable is not defined on the sole Hilbert space of the signal mode [1]. Rather, it reflects properties of the global state which results from the interaction among the signal mode and the set of the probe modes. In some cases, it is possible to get rid of the probe modes, such that the statistics of the output depends only on the quantum statistics of the signal mode. This is for example the case of balanced homodyne detectors [2], where an appropriate rescaling of the output photocurrent permits to completely neglect the local oscillator from the definition of the measured observable, which is proportional to the signal field quadrature $\hat{a}(\phi) = \frac{1}{2}(a^\dagger e^{i\phi} + a e^{-i\phi})$.

This procedure, however, cannot be generalized to any setup and, in general the output statistics of a detector always depends on how we are probing the signal under examination. In quantum optics this is a common feature of three relevant detection schemes, which provide three different setup for the joint measurement of a couple of photocurrents. They are the heterodyne [3–5], the eight-port homodyne [6,7] and the six-port homodyne detectors [8,9]. The main goal of this paper is to show that although they involve different ways of coupling the signal to the probe, they provide the same information on the signal under examination. Actually, we will prove their full equivalence by demonstrating that their output photocurrents have the same operatorial form. Remarkably, such equivalence still holds when we take into account the quantum efficiency of the photodetection, even though this process occurs at different stages in the three detection schemes.

The relevance of two-photocurrent detectors stems from their versatility in the characterization of quantum states of the radiation field. In fact, the outcomes from a two-photocurrent detector are couples of real numbers that are distributed according to a bidimensional density $K(x,y)$ which is given by the convolution of the signal and the probe Wigner functions. This means that *quantum filtering* of the signal Wigner function is allowed, and that this process can be used to enhance sensitivity in the detection of specific feature of the signal, such that the amplitude or the phase. In other words, two-photocurrent detectors permits to manipulate and redirect quantum fluctuations.

The paper is organized as follows. In the next section we briefly review how to describe inefficient photodetection in terms of beam splitters and ideal detectors. In Sections III, IV, and V we prove the equivalence of heterodyne, eight-port homodyne, and six-port homodyne detectors by showing that they jointly measure the real and the imaginary part of the complex photocurrent $\widehat{\mathcal{Z}} = a + b^\dagger$, a being the signal mode and b a probe mode. The inefficiency of realistic photodetectors will be also taken into account, in order to show that it does not affect the equivalence of the schemes. In section VI we derive the output statistics of two-photocurrent devices and show how to use such schemes for *quantum filtering* of the signal Wigner function. Section VII will close the paper with some concluding remarks.

II. INEFFICIENT PHOTODETECTION

The final stage of any detection scheme is represented by photodetection, namely counting photon through their conversion to electric pulses. Let us consider a light beam $\hat{\rho}$ entering a phototube which converts to electric pulses only a fraction ζ of the incoming photons. By opening the detector window for a time interval T, the probability $P_m(T)$ of counting m photons is given by [10]

$$P_m(T) = \mathrm{Tr}\left\{\hat{\rho}{:}\frac{[\zeta\hat{I}(T)T]^m}{m!}\exp[-\zeta\hat{I}(T)T]{:}\right\}\ , \tag{1}$$

where $: \; :$ denotes normal ordering of operator and $\hat{I}(T)$ is the beam intensity

$$\hat{I}(T) = \frac{2\epsilon_0 c}{T} \int_0^T \hat{\mathbf{E}}^{(-)}(\mathbf{r},t) \cdot \hat{\mathbf{E}}^{(+)}(\mathbf{r},t) dt \; . \tag{2}$$

$\hat{\mathbf{E}}^{(\pm)}(\mathbf{r},t)$ denotes the positive (negative) frequency part of the field. For a single-mode field excited in a stationary state Eq. (1) can be rewritten as

$$P_m^\eta = \mathrm{Tr}\left\{ \hat{\rho} \, \frac{(\eta a^\dagger a)^m}{m!} \exp(-\eta a^\dagger a) \right\} \; , \tag{3}$$

$[a, a^\dagger] = 1$ being the single mode field operator and $\eta = \zeta c \hbar \omega / V$ the global quantum efficiency of the photodetectors. For unit quantum efficiency this coincides with the actual photon number distribution of the state under examination

$$P_m^1 = \rho_{mm} \equiv \langle m | \hat{\rho} | m \rangle \; , \tag{4}$$

whereas, in the realistic case of non-unit quantum efficiency Eq. (3) becomes a binomial convolution [11]. In formula

$$P_m^\eta = \sum_{n=m}^{\infty} \rho_{nn} \left(\begin{array}{c} n \\ m \end{array} \right) \eta^m (1-\eta)^{n-m} \; . \tag{5}$$

Let us now consider the scheme in Fig. 1. The signal mode a is impinged in a beam splitter of transmissivity τ whose second port b is placed in the vacuum. A perfect ($\eta = 1$) photodetection on the exiting mode reveals m photons with a probability

$$P_m = \mathrm{Tr}\left[\hat{U}_\tau (\hat{\rho} \otimes |0\rangle\langle 0|) \hat{U}_\tau^\dagger \, |m\rangle\langle m| \otimes \mathbb{I} \right] \; , \tag{6}$$

$\mathbb{I}$ being the identity operator on the second input and

$$\hat{U}_\tau = \exp\left\{ i \arctan\sqrt{\frac{1-\tau}{\tau}} \left(a^\dagger b + a b^\dagger \right) \right\} \; ,$$

the evolution operator of the beam splitter.
A straightforward calculation shows that

$$P_m = \sum_{n=m}^{\infty} \rho_{nn} \left(\begin{array}{c} n \\ m \end{array} \right) (1-\tau)^{n-m} \tau^m \; . \tag{7}$$

Eq. (7) coincides with Eq. (5) for $\tau = \eta$. This means that a photodetection process with efficiency η is equivalent to a perfect photodetection process performed on the original signal mixed with vacuum by a beam splitter with a value of the transmissivity equal to the quantum efficiency [12,13]. In the following we will adopt this equivalent scheme.

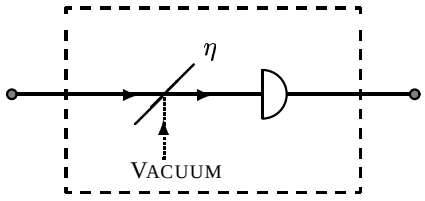

FIG. 1. Scheme for inefficient photodetection.

III. EIGHT-PORT HOMODYNE DETECTOR

Eight-port homodyne detector is known for a long time for the joint determination of phase and amplitude of the field in the microwave domain, and it was subsequently introduced in the optical domain [6,7,14]. A schematic diagram of the experimental setup is reported in Fig. 2. There are four balanced beam splitters whereas a $\pi/2$ phase shifter is inserted in one arm. The four input modes are denoted by a_k, $k = 1, ..., 4$ whereas the detected output modes are denoted by b_k, $k = 1, ..., 4$. There are four identical photodetectors whose quantum efficiency is given by η. The *noise* modes used to take into account inefficiency, according to the scheme of the previous section, are denoted by u_i, $i = 1, ..., 4$. We consider a_1 as the signal mode, whereas a_2 is referred to be the idler of the device. The mode a_3 is unexcited, whereas a_4 is placed in a highly excited coherent state $|z\rangle$ provided by an intense laser beam (local oscillator). The detected photocurrents are $\hat{I}_k = b_k^\dagger b_k$, $k = 1, ..., 4$ which form the eight-port homodyne observables

$$\widehat{\mathcal{Z}}_1 = \frac{\hat{I}_2 - \hat{I}_1}{2\eta|z|} \qquad \widehat{\mathcal{Z}}_2 = \frac{\hat{I}_4 - \hat{I}_3}{2\eta|z|} \,. \tag{8}$$

The latter are derived by rescaling the difference photocurrent, each of them obtained in an homodyne scheme. For this reason eight-port homodyne is known also as double-homodyne detection. In Eq. (8) η denotes the quantum efficiency of the photodetectors whereas $|z|$ is the intensity of the local oscillator. In order to obtain $\widehat{\mathcal{Z}}_1$ and $\widehat{\mathcal{Z}}_2$ in terms of the input modes we first note that the input-output mode transformation is necessarily linear, as only passive components are involved in the detection scheme. Thus, we can write

$$b_k = \sum_{l=1}^{4} M_{kl} a_l \,, \tag{9}$$

where the transformation matrix can be computed starting from the corresponding transformations for the beam splitters and the phase shifter [17]

$$\mathbf{M} = \frac{1}{\sqrt{4}} \begin{bmatrix} 1 & 1 & 1 & 1 \\ 1 & i & -1 & -i \\ 1 & -1 & i & -1 \\ 1 & -i & -1 & i \end{bmatrix} \,. \tag{10}$$

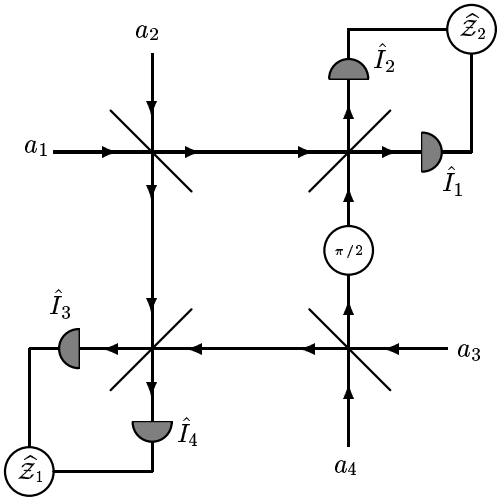

FIG. 2. Schematic diagram of an eight-port homodyne detector.

Eqs. (9) and (10) together with the equivalent scheme for the inefficient detector leads to the following expression for the output modes

$$\begin{aligned} b_1 &= \sqrt{\eta}\,[a_1 + a_2 + a_3 + a_4] + \sqrt{1-\eta}\,u_1 \\ b_2 &= \sqrt{\eta}\,[a_1 + ia_2 - a_3 - ia_4] + \sqrt{1-\eta}\,u_2 \\ b_3 &= \sqrt{\eta}\,[a_1 - a_2 + ia_3 - a_4] + \sqrt{1-\eta}\,u_3 \\ b_4 &= \sqrt{\eta}\,[a_1 - ia_2 - a_3 + ia_4] + \sqrt{1-\eta}\,u_4 \,. \end{aligned} \tag{11}$$

Upon inserting Eqs. (11) in Eq. (8), and by considering the limit of highly excited local oscillator, we obtain the eight-port photocurrents in terms of the input modes

$$\begin{aligned} \widehat{\mathcal{Z}}_1 &= \hat{a}_1(0) + \hat{a}_2(0) + \sqrt{\frac{1-\eta}{\eta}}\,[\hat{u}_1(0) - \hat{u}_2(0)] + O[\frac{1}{|z|}] \\ \widehat{\mathcal{Z}}_2 &= -\hat{a}_1(\pi/2) + \hat{a}_2(\pi/2) + \sqrt{\frac{1-\eta}{\eta}}\,[\hat{u}_3(\pi/2) - \hat{u}_4(\pi/2)] + O[\frac{1}{|z|}] \,. \end{aligned} \tag{12}$$

In Eq. (12) $\hat{a}(\phi)$ denotes a quadrature of the field. For unit quantum efficiency, the complex photocurrent $\mathcal{Z} = \mathcal{Z}_1 + i\mathcal{Z}_2$ is given by

$$\mathcal{Z} = a_1 + a_2^\dagger \,, \tag{13}$$

whereas for non unit quantum efficiency it becomes a Gaussian convolution of Eq. (13), we will consider this point in detail in VI.

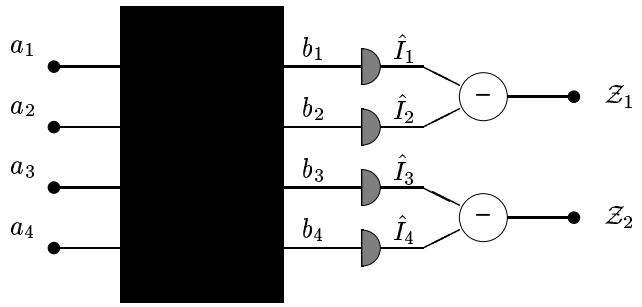

FIG. 3. Eight-port homodyne detector as a multiport homodyne.

It is worth noticing here that the mode transformation defined by Eqs. (9) and (10) is distinctive for a canonical 4×4-port linear coupler as defined in Refs. [15,16]. It has been rigorously shown [17] that a $N \times N$-port linear coupler can always be realized in terms of a number of beam splitters and phase-shifters. However, this implementation is, in general, not unique. The interest of eight-port homodyne scheme lies in the fact it provides the minimal scheme for realizing a 4×4-multiport [18]. If one considers the multiport as a given *black-box* device the eight-port homodyne scheme can be depicted as in Fig. 3. This will facilitate the comparison with the six-port homodyne detection presented in Section V.

IV. HETERODYNE DETECTOR

Heterodyne detection scheme is known for a long time in radiophysics. It has been introduced in the domain of optics [3–5,19] in order to describe the joint measurement of two conjugated quadratures of the field. The term 'heterodyne' comes from the fact that the involved modes are excited on different frequencies.

In Fig. 4 we show a schematic diagram of the detector. We denote by $\hat{\mathbf{E}}_S$ the signal field, whereas $\hat{\mathbf{E}}_{LO}$ describes the local oscillator. The field $\hat{\mathbf{E}}_L$ accounts for the losses due to inefficient photodetection. The input signal is excited in a single mode (say a) at the frequency ω, as well as the local oscillator which is excited at a mode at the frequency ω_0. This local oscillator mode is placed in a strong coherent state $|z\rangle$ by means of an intense laser beam. The beam splitter has a transmissivity given by τ, whereas the photodetectors shows quantum efficiency η.

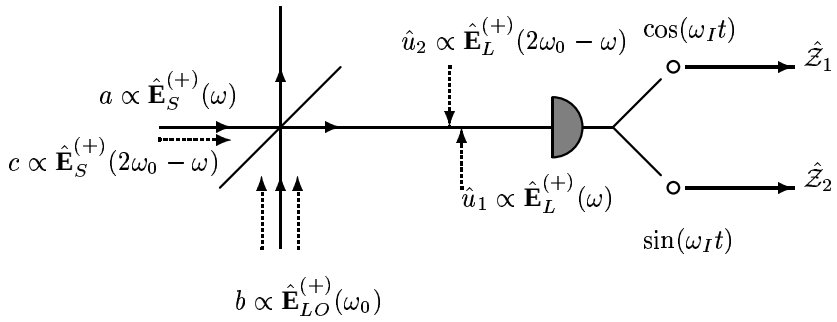

FIG. 4. Schematic diagram of a heterodyne detection. Relevant modes are explicitly pointed out.

The heterodyne output photocurrents are given by the real $\widehat{\mathcal{Z}}_1$ and the imaginary $\widehat{\mathcal{Z}}_2$ part of the complex photocurrent $\widehat{\mathcal{Z}}$. The latter is obtained after the rescaling of the output photocurrent $\hat{I}$, which is measured at the intermediate frequency $\omega_I = \omega - \omega_0$. By Fourier transform of Eq. (2) we have

$$\hat{I}(\omega_I) = \int_{\mathbf{R}} d\omega' \, \hat{\mathbf{E}}_O^{(-)}(\omega' + \omega_I) \, \hat{\mathbf{E}}_O^{(+)}(\omega') \,, \tag{14}$$

$\hat{\mathbf{E}}_O^{(\pm)}$ being the positive and the negative part of the output field. In terms of the input fields Eq. (14) can be written as

$$\hat{I}(\omega_I) = \int_{\mathbf{R}} d\omega' \Big[\sqrt{\eta\tau}\hat{\mathbf{E}}_S^{(-)}(\omega' + \omega_I) + \sqrt{\eta(1-\tau)}\hat{\mathbf{E}}_{LO}^{(-)}(\omega' + \omega_I) + \sqrt{1-\eta}\hat{\mathbf{E}}_L^{(-)}(\omega' + \omega_I) \Big]$$
$$\Big[\sqrt{\eta\tau}\hat{\mathbf{E}}_S^{(+)}(\omega') + \sqrt{\eta(1-\tau)}\hat{\mathbf{E}}_{LO}^{(+)}(\omega') + \sqrt{1-\eta}\hat{\mathbf{E}}_L^{(+)}(\omega') \Big] \ . \tag{15}$$

Heterodyne photocurrent is obtained by the following rescaling

$$\widehat{\mathcal{Z}} = \lim_{\tau \to 1, |z| \to \infty} \frac{\hat{I}(\omega_I)}{|z|\eta\sqrt{\tau(1-\tau)}} \qquad \text{with } |z|\sqrt{1-\tau} \text{ constant} \ . \tag{16}$$

In practice, this definition corresponds to have a very intense local oscillator, which is allowed only for a little mixing with the signal mode [20]. In this limit only terms containing the local oscillator field $\mathbf{E}_{LO}^{(\pm)}(\omega_0)$ at the frequency ω_0 can survive in Eq. (15), so that we have

$$\widehat{\mathcal{Z}} = \widehat{\mathcal{Z}}_1 + i\,\widehat{\mathcal{Z}}_2 \ , \tag{17}$$

where

$$\widehat{\mathcal{Z}}_1 = \hat{a}(0) + \hat{c}(0) + \sqrt{\frac{1-\eta}{\eta}}\ (\hat{u}_1(0) - \hat{u}_2(0))$$
$$\widehat{\mathcal{Z}}_2 = -\hat{a}(\pi/2) + \hat{c}(\pi/2) + \sqrt{\frac{1-\eta}{\eta}}\ (\hat{u}_1(\pi/2) - \hat{u}_2(\pi/2)) \ . \tag{18}$$

In writing Eq. (18) we have substituted

$$c \leftarrow \hat{\mathbf{E}}_S^{(+)}(2\omega_0 - \omega) \qquad u_1 \leftarrow \hat{\mathbf{E}}_L^{(+)}(\omega) \qquad u_2 \leftarrow \hat{\mathbf{E}}_L^{(+)}(2\omega_0 - \omega) \tag{19}$$

for the relevant modes involved. Since u_1 and u_2 are not excited, they play the role of noise modes accounting for the quantum efficiency of the photodetector. The expression (18) for the heterodyne photocurrents is thus equivalent to that of Eq. (12) for the eight-port homodyne scheme, the mode c playing the role of the idler of the device. The full equivalence of the two detection schemes has been thus proved.

V. SIX-PORT HOMODYNE DETECTOR

A linear, symmetric three-port optical coupler is a straightforward generalization of the customary lossless symmetric beam splitter. The three input modes a_i, $i = 1,2,3$ are combined to form 3 output modes b_j, $j = 1,2,3$. In analogy to lossless beam splitters, which are described by unitary 2×2 matrices [21], any lossless triple coupler is characterized by a unitary 3×3 matrix [22,23]. For the symmetric case we have the form

$$\mathbf{T} = \frac{1}{\sqrt{3}} \begin{pmatrix} 1 & 1 & 1 \\ 1 & \exp\{i\frac{2\pi}{3}\} & \exp\{-i\frac{2\pi}{3}\} \\ 1 & \exp\{-i\frac{2\pi}{3}\} & \exp\{i\frac{2\pi}{3}\} \end{pmatrix} \ , \tag{20}$$

where each matrix element T_{ij} represents the transmission amplitude from the i-th input port to the j-th output port, that is $b_j = \sum_{k=1}^{3} T_{jk} a_k$. Such devices have already been implemented in single-mode optical fiber technology and commercial triple coupler are available [24]. Any triple coupler can be also implemented by discrete optical components using symmetric beam splitters and phase shifters only [22]. As it has already mentioned in Section III, this is due to the fact that that any unitary M-dimensional matrix can be factorized into a sequence of 2-dimensional transformations plus phase-shifts [17]. Moreover, this decomposition is not, in general, unique. In Fig. 5 a possible implementation of a triple coupler is schematically reported.

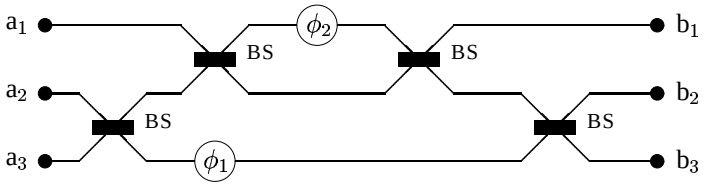

FIG. 5. Realization of a triple coupler in terms of 50:50 beam splitters (BS) and phase shifters 'ϕ'. In order to obtain a symmetric coupler the following values has to be chosen: $\phi_1 = \arccos(1/3)$ and $\phi_2 = \phi_1/2$.

Experimental realizations of triple couplers has been reported for both cases, the passive elements case and the optical fiber one [22,23,25,26]. Let us now consider the measurement scheme of Fig. 6. The three input modes are mixed by a triple coupler and the resulting output modes are subsequently detected by three identical photodetectors. The measured photocurrents are proportional to $\hat{I}_n$, $n = 1, 2, 3$ given by

$$\hat{I}_n = b_n^\dagger b_n = \frac{1}{3}\sum_{k,l=1}^{3} \exp\{i\theta_n(l-k)\}\, a_k^\dagger a_l \ , \qquad \theta_n = \frac{2\pi}{3}(n-1) \ . \tag{21}$$

After photodetection a Fourier transform (FT) on the photocurrents is performed

$$\hat{\mathcal{I}}_s \equiv \mathrm{FT}(\hat{I}_1, \hat{I}_2, \hat{I}_3) = \frac{1}{\sqrt{3}}\sum_{n=1}^{3} \hat{I}_n \exp\{-i\theta_n(s-1)\} \ , \qquad s = 1, 2, 3 \, . \tag{22}$$

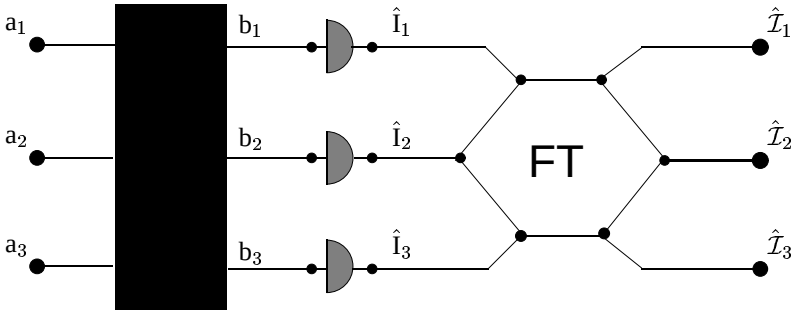

FIG. 6. Outline of triple coupler homodyne detectors: The hexagonal box symbolizes the electronically performed Fourier transform (FT).

This procedure is a straightforward generalization of the customary two-mode balanced homodyning technique. In that case, in fact, the sum and the difference of the two output photocurrents are considered, which actually represent the Fourier transform in a two-dimensional space. By means of the identity

$$\delta_3(s-1) = \frac{1}{3}\sum_{n=1}^{3} \exp\left\{i\frac{2\pi}{3}n(s-1)\right\} \ , \tag{23}$$

for the periodic (modulus 3) Kronecker delta δ_3, we obtain our final expressions for the Fourier transformed photocurrents

$$\hat{\mathcal{I}}_1 = \frac{1}{\sqrt{3}}\left\{a_1^\dagger a_1 + a_2^\dagger a_2 + a_3^\dagger a_3\right\} \ , \tag{24}$$

$$\hat{\mathcal{I}}_2 = \frac{1}{\sqrt{3}}\left\{a_1^\dagger a_2 + a_2^\dagger a_3 + a_3^\dagger a_1\right\} \ , \tag{25}$$

$$\hat{\mathcal{I}}_3 = \frac{1}{\sqrt{3}}\left\{a_1^\dagger a_3 + a_2^\dagger a_1 + a_3^\dagger a_2\right\} \ . \tag{26}$$

$\hat{\mathcal{I}}_1$ gives no relevant information as it is insensitive to the phase of the signal field, whereas $\hat{\mathcal{I}}_2$ and $\hat{\mathcal{I}}_3$ are hermitian conjugates of each other and contain the relevant information in their real and imaginary part. In the following let us assume a_1 is the signal mode and a_2 is fed by a highly excited coherent state $|z\rangle$ representing the local oscillator. For large $|z|$ the output photocurrents are intense enough to be easily detected. They can be combined to give the reduced photocurrents

$$\begin{aligned} \hat{\mathcal{Z}}_1 &= \sqrt{3}\frac{\hat{\mathcal{I}}_2 + \hat{\mathcal{I}}_3}{2|z|} = \hat{a}_1(0) + \hat{a}_3(0) + O[\frac{1}{|z|}] \\ \hat{\mathcal{Z}}_2 &= \sqrt{3}\frac{\hat{\mathcal{I}}_2 - \hat{\mathcal{I}}_3}{2i|z|} = -\hat{a}_1(\pi/2) + \hat{a}_3(\pi/2) + O[\frac{1}{|z|}] \, , \end{aligned} \tag{27}$$

which we refer to as the *triple homodyne photocurrents*. Again the complex photocurrent $\hat{\mathcal{Z}} = \hat{\mathcal{Z}}_1 + i\hat{\mathcal{Z}}_2$ has the form $\hat{\mathcal{Z}} = a_1 + a_3^\dagger$, a_1 being the signal mode and a_3 the idler of the device.

When accounting for the non unit quantum efficiency η of the photodetectors the output modes are written as

$$b_j = \sqrt{\eta}\,\left(\sum_{k=1}^{3} T_{jk} a_k\right) + \sqrt{1-\eta}\,u_j \qquad j = 1,2,3\,,$$

so that the reduced photocurrents are now given by

$$\widehat{\mathcal{Z}}_1 = \sqrt{3}\frac{\hat{\mathcal{I}}_2 + \hat{\mathcal{I}}_3}{2\eta|z|} = \hat{a}_1(0) + \hat{a}_3(0) + \sqrt{\frac{1-\eta}{\eta}}\,[\hat{u}_1(0) - \hat{u}_3(0)] + O[\frac{1}{|z|}]$$
$$\widehat{\mathcal{Z}}_2 = \sqrt{3}\frac{\hat{\mathcal{I}}_2 - \hat{\mathcal{I}}_3}{2i\eta|z|} = -\hat{a}_1(\pi/2) + \hat{a}_3(\pi/2) + \sqrt{\frac{1-\eta}{\eta}}\,[\hat{u}_1(\pi/2) - \hat{u}_3(\pi/2)] + O[\frac{1}{|z|}]\,. \tag{28}$$

When, as it is the case, the modes u_j are placed in the vacuum the six-port photocurrents in Eq. (28) leads to the same statistics of the eight-port photocurrents in Eq. (12). Indeed, they describe different devices leading to the same amount of information on the signal mode a_1. Some comments are, however, in order. By comparison of Fig. 3 and Fig. 6 it appears obvious that six-port homodyne is an optimized scheme relative to the eight-port one. One mode less is needed to reach the same amount of information, thus decreasing the possible sources of noise. The reason for this lies in the final stage of the two schemes. The Fourier transform of the six-port photocurrents, in fact, is a more effective procedure relative to the double-homodyne final stage of the eight-port scheme. This is related to the noise suppression mechanism of homodyne detection. The latter, in fact, is generalized to the multi-mode case by the Fourier transform rather than duplication of the original two-mode scheme.

VI. OUTPUT STATISTICS FROM A TWO-PHOTOCURRENT DEVICE

In this section we analyze with some detail the output statistics of an abstract two-photocurrent device. The latter is characterized by the joint measurement of the real $\widehat{\mathcal{Z}}_1$ and the imaginary $\widehat{\mathcal{Z}}_2$ part of the complex photocurrent

$$\widehat{\mathcal{Z}} = a + b^\dagger\,, \tag{29}$$

when equipped with perfect photodetectors. On the other hand, in the realistic case of inefficient photodetection the photocurrent is given by

$$\widehat{\mathcal{Z}} = a + b^\dagger + \sqrt{\frac{1-\eta}{\eta}}\left(u_1 + u_2^\dagger\right)\,. \tag{30}$$

In Eqs. (29) and (30) a and b denote single mode radiation field which can be excited in any quantum state, whereas u_1 and u_2 denote mode placed in the vacuum that are used to describe losses due inefficient photodetection, according to the equivalent detection scheme of Section II. In the following we will refer to the mode a as the signal mode which is under examination, whereas the mode b is in excited in a known, and fixed state, playing the role of the probe mode of the device. Of course, This is only for the sake of convenience, since the roles of the two modes can be exchanged, and any argument can be reversed considering the mode b as a signal mode. We denote the outcome probability density distribution by $K(\alpha,\bar{\alpha})$, which describes, in the complex plane, the state of the mode a as probed by the mode b. Different choices for the probe mode lead to different features of the probability distribution.

Each experimental random outcome (z_1, z_2) from the joint measurement of $\widehat{\mathcal{Z}}_1$ and $\widehat{\mathcal{Z}}_2$ can be considered as a point z in the complex plane. On the other hand, the output photocurrent $\widehat{\mathcal{Z}}$ is expressed as a sum of different contributions coming from different modes. Therefore, it appears rather intuitive that the resulting probability distribution will be given by a convolution. In oder to be more specific, let us start by considering the ideal case of unit quantum efficiency $\eta = 1$. We write the probability distribution $K(\alpha)$ as the Fourier transform [1]

$$K(\alpha) = \int_{\mathbf{C}} \frac{d^2\gamma}{\pi^2}\, e^{\bar{\gamma}\alpha - \gamma\bar{\alpha}}\, \Xi(\gamma)\,, \tag{31}$$

of the characteristic function

[1] As a matter of fact, the outcome are distributed according to an analytic function $K(\alpha,\bar{\alpha})$ of both variable α and $\bar{\alpha}$. In the following, for the sake of simplicity, we leave the dependence on $\bar{\alpha}$ implicit.

$$\Xi(\gamma) = \mathrm{Tr}\left\{\hat{\varrho}\,\exp\left[\bar{\gamma}\widehat{\mathcal{Z}} - \gamma\widehat{\mathcal{Z}}^{\dagger}\right]\right\}\,, \tag{32}$$

$\hat{\varrho}$ being the global density matrix describing both modes a and b. We consider probe mode to be independent on the signal mode, so that the input mode is factorized as

$$\hat{\varrho} = \hat{\varrho}_a \otimes \hat{\varrho}_b\,. \tag{33}$$

Upon substituting Eqs. (29) and (33) in Eq. (32) we are able to write the characteristic function $\Xi(\gamma,\bar{\gamma})$ as a product

$$\Xi(\gamma) = \mathrm{Tr}\left\{\hat{\varrho}_a \otimes \hat{\varrho}_b\;\; \hat{D}_a(\gamma)\otimes\hat{D}_b(-\gamma)\right\} = \chi_a(\gamma)\;\chi_b(-\gamma)\,, \tag{34}$$

$$\hat{D}(\gamma) = \left\{\hat{\rho}\exp\left[\gamma a^{\dagger} - \bar{\gamma}a\right]\right\}$$

being the displacement operator and

$$\chi(\gamma) = \mathrm{Tr}\left\{\hat{\varrho}\,\hat{D}(\gamma)\right\}$$

the single mode characteristics function, the latter entering in the definition of the Wigner function of a single mode radiation field [27–29]

$$W(\alpha) = \int \frac{d^2\lambda}{\pi}\,\chi(\lambda)\;\exp\left\{\bar{\lambda}\alpha - \lambda\bar{\alpha}\right\}\,. \tag{35}$$

We now insert Eq. (34) in Eq. (31). By means of Eq. (35) and using the convolution theorem we arrive at the final result

$$K(\alpha) = W_a(\alpha,)\;\star\;W_b(-\alpha) = \int_{\mathbf{C}}\frac{d^2\beta}{\pi^2}\,W_b(\alpha+\beta)\,W_a(\beta)\,, \tag{36}$$

the symbol $\star$ denoting convolution. Eq. (36) is the basis for referring to the mode b as the probe of the device. Its action, in fact, is that of filtering on signal Wigner function, which itself is not a genuine probability distribution, since it can exhibit negative values. Indeed, the Wigner function, though it contains a complete description of the quantum state, cannot be directly measured, *i.e.* sampled by experiments. However, the convolution (36) make it a regular positive definite distribution, leading to $K(\alpha)$ which is a measurable distribution.

Phase space density as in Eq. (36) have been already introduced by Wodkiewicz [30] to account for the effect of the measuring apparatus in a joint measurement of conjugated variables. Two-photocurrent devices appear as the natural setup to start from, in order to experimentally access such kind of phase-space distribution.

The phase-space distributions $K(\alpha)$ are smoothed (broader) versions of the Wigner function, corresponding to the occurrence of additional noise of purely quantum origin. In fact, two-photocurrent devices provide the generalized joint measurement of position and momentum, thus unavoidably introducing additional noise according to uncertainty relations [19,31,32]. The crucial point however, is that two-photocurrent devices offer the possibility to manipulate such quantum noise. As it emerges from Eq. (36) the noise can be redirected into the desidered region of the phase space by a suitable choice of the probe mode, according to the kind of information which is of interest.

In order to incorporate the effects of inefficient detection we first note that Eq. (30) differs from Eq. (29) by two additional *additive* terms. Therefore, further convolutions to the original Wigner function are expected. Indeed, the characteristic function in presence of detection losses is given by

$$\Xi_\eta(\gamma) = \chi_a(\gamma)\;\chi_b(-\gamma)\,\chi_{u_1}\left(\sqrt{\frac{1-\eta}{\eta}}\,\gamma\right)\;\chi_{u_2}\left(-\sqrt{\frac{1-\eta}{\eta}}\,\gamma\right) \tag{37}$$

where characteristic function for the noise modes can be easily evaluated as

$$\chi_{u_j}\left(-\sqrt{\frac{1-\eta}{\eta}}\gamma\right) = \exp\left[-\frac{1-\eta}{2\eta}\,|\gamma|^2\right] \qquad j=1,2\,. \tag{38}$$

Upon inserting Eqs. (37) and (38) in Eq. (31) we obtain our final result, namely the output probability distribution $K_\eta(\alpha)$ of a two-photocurrent device equipped with photodetectors of quantum efficiency η

$$K_\eta(\alpha) = K(\alpha)\;\star\;G_\eta(\alpha) = \int_{\mathbf{C}}\frac{d^2\beta}{\pi^2}\,K(\beta)\,G_\eta(\alpha-\beta)\,, \tag{39}$$

where $K(\alpha)$ is the probability distribution obtained for ideal photodetection and

$$G_\eta(\alpha) = \exp\left[-\frac{\eta}{1-\eta}|\alpha|^2\right]$$

the filter function summarizing the effects of inefficient photodetection.

A. Probabbility operator measure of two-photocurrent devices

Starting from Eqs. (31) and (32) it easy to rewrite the distribution $K(\alpha)$ as

$$K(\alpha) = \mathrm{Tr}\left[\hat{\varrho}_a\, \mu(\alpha)\right] \ , \tag{40}$$

where

$$\mu(\alpha) = D_b(\alpha)\hat{\varrho}_b D_b^\dagger(\alpha)$$

represents the probability operator-valued measure (POvM) of the apparatus. The filtering action of the probe is reflected into the dependence of $\mu(\alpha)$ on the probe state $\hat{\varrho}_b$. For nonunit quantum efficiency we have $K_\eta(\alpha) = \mathrm{Tr}\left[\hat{\varrho}_a\, \mu_\eta(\alpha)\right]$ with

$$\mu_\eta(\alpha) = \int_{\mathbf{C}} \frac{d^2\beta}{\pi^2}\, \mu(\beta)\, G_\eta(\alpha-\beta) \ . \tag{41}$$

B. Quantum filtering

The simplest choice for the probe mode is given by the vacuum state, whose Wigner function is given by $W_{\mathrm{VAC}}(\alpha) = (2/\pi)^{1/2}\exp[-2|\alpha|^2]$. The corresponding output distribution is thus given by $K(\alpha) = W(\alpha) \star W_{\mathrm{VAC}}(\alpha)$, which coincides with the Husimi Q function $Q(\alpha) = 1/\pi\langle\alpha|\hat{\varrho}|\alpha\rangle$. Compared to the Wigner function, the Q function is a broader distribution, with the broadening that accounts for the additional noise introduced by the joint measurement or, in other words, due to the vacuum fluctuations introduced by the probe. We remind that generalized Wigner functions are defined as the convolution $W_s(\alpha) = W(\alpha) \star G_{(1-s)^{-1}}(\alpha)$ The Wigner function itself is obtained for $s = 0$, and the Husimi Q function for $s = -1$. If the probe is excited by a squeezed state the resulting distribution is squeezed accordingly. This feature has been used to devise an optimized two-step measurement for the precise measurement of a phase-shift [33].

VII. CONCLUSIONS

In this paper we have introduced the class of two-photocurrent devices. This kind of detectors are characterized by the fact that they jointly measure the real and the imaginary part of the complex photocurrent $\mathcal{Z} = a + b^\dagger$, where a and b describe two single mode of the radiation field. Eight-port homodyne, heterodyne and six-port homodyne detectors belong to this general class, thus their fully equivalence in probing radiation field has been proved. It has also been proved that this equivalence still holds when the inefficiency of the photodetection process is taken into account. This is an interesting and partially unexpected result, since photodetection takes place at very different stages in the three detection schemes.

The three schemes analyzed in this paper are equivalent from the point of view of provided information on the measured signal. Nevertheless, they have different physical implementations which have to be compared. We pointed out the advantages of the six-port homodyne scheme in comparison with the customary eight-port one. Actually, it provides the minimal scheme to access generalized phase space distribution.

In a two-photocurrent device a generalized joint measurement of position and momentum is performed on the signal mode. This results in a smoothing of the signal Wigner function to a measurable distribution, which represents the output probability distribution of the measurement. Some additional noise is unavoidably introduced, according to the Heisenberg principle for joint measurement. However, the filtering process has been shown to be a convolution with the Wigner function of the probe mode. Therefore, it is possible to manipulate and redirect the noise. A suitable choice of the probe mode enhances different features of the signal' phase space distribution, according to the kind of desidered information.

[1] Busch P, Lahti P J 1995 *Riv. Nuovo Cim.* **18** 1
[2] Yuen H P, Chan V W S 1983 *Opt. Lett.* **8** 177
[3] Yuen H P, Shapiro J H 1980 *IEEE Trans. Inf. Theory* **IT-26** 78
[4] Shapiro J H, Wagner S S 1984 *IEEE J. Quant. Electron.* **QE-20** 803

[5] Shapiro J H 1985 *IEEE J. Quant. Electron.* **QE-21** 237
[6] Walker N G 1987 *J. Mod. Opt.* **34** 15
[7] Lai Y, Haus H A 1989 *Quantum Opt.* **1** 99
[8] Paris M G A, Chizhov A, Steuernagel O 1996 *Opt. Comm.***134** 117
[9] Zucchetti A, Vogel W, Welsch D G 1996 *Phys. Rev.* A**54** 856
[10] Kelley P L, Kleiner W H, 1964 *Phys. Rev.* **136** 316
[11] Mandel L, Wolf E 1995 *Optical Coherence and Quantum Optics*, (Cambridge University Press)
[12] Leonhardt U, Paul H 1993 *Phys. Rev.* A**48** 4598
[13] D'Ariano G M, Macchiavello C, Paris M G A 1995 *Phys. Lett.* A**198** 286
[14] Noh J W, Fougeres A, Mandel L 1991 *Phys. Rev. Lett.* **67** 1426
[15] Törmä P, Stenholm S, Jex I 1995 *Phys. Rev.* A**52** 4853
[16] Jex I, Stenholm S, Zeilinger A 1995 *Opt. Comm.* **117** 95
[17] Reck M, Zeilinger A, Bernstein H J, Bertani P 1994 *Phys. Rev. Lett.* **73** 58
[18] Törmä P, Jex I, Stenholm S 1996 *J. Mod. Opt.* **43** 245
[19] Yuen H P 1982 *Phys. Lett.* A**91** 101
[20] Paris M G A 1996 *Phys. Lett.* A**217** 78
[21] Campos R A, Saleh B E A, Teich M C 1989 *Phys. Rev.* A**40**1371
[22] Mattle K, Michler M, Weinfurther H, Zeilinger A, Zukowski M 1995 *Appl. Phys.* B**60** S111
[23] Weihs G, Reck M, Weinfurther H, Zeilinger A 1996 *Opt. Lett.* **21** 302
[24] Sheem S K 1981 *J. Appl. Phys.* **52** 3865
[25] Hariharan P, Sen D 1959 *J. Sci. Instr. 36* 70
[26] Zernike F 1950 *J. Opt. Soc. Am.* **40** 326
[27] Wigner E P 1932 *Phys. Rev.* **40** 749
[28] Cahill K E, Glauber R J 1969 *Phys. Rev.* **177** 1857
[29] Cahill K E, Glauber R J 1969 *Phys. Rev.* **177** 1882
[30] Wodkiewicz K 1984 *Phys. Rev. Lett.* **52** 1064
[31] She C Y, Heffner H 1966 *Phys. Rev.* **152** 1103
[32] Arthurs E, Goodman M S 1988 *Phys. Rev. Lett.* **60** 2447
[33] A. V. Chizhov, V. De Renzi, M. G. A. Paris, Phys. Lett. A **237** 201 (1998).